Superscaling, scaling functions, and nucleon momentum distributions in nuclei

A. N. Antonov,[1] M. K. Gaidarov,[1] M. V. Ivanov,[1] D. N. Kadrev,[1] E. Moya de Guerra,[2] P. Sarriguren,[2] and J. M. Udias[3]
[1]*Institute for Nuclear Research and Nuclear Energy, Bulgarian Academy of Sciences, Sofia 1784, Bulgaria*
[2]*Instituto de Estructura de la Materia, CSIC, Serrano 123, E-28006 Madrid, Spain*
[3]*Departamento de Fisica Atomica, Molecular y Nuclear, Facultad de Ciencias Fisicas, Universidad Complutense de Madrid, E-28040 Madrid, Spain*
(Received 21 October 2004; published 27 January 2005)

The scaling functions $f(\psi')$ and $F(y)$ from the ψ'- and y-scaling analyses of inclusive electron scattering from nuclei are explored within the coherent density fluctuation model (CDFM). In addition to the CDFM formulation in which the local density distribution is used, we introduce a new equivalent formulation of the CDFM based on the one-body nucleon momentum distribution (NMD). Special attention is paid to the different ways in which the excitation energy of the residual system is taken into account in y and ψ' scaling. Both functions, $f(\psi')$ and $F(y)$, are calculated using different NMDs and compared with the experimental data for a wide range of nuclei. The good description of the data for $y < 0$ and $\psi' < 0$ (including $\psi' < -1$) makes it possible to show the sensitivity of the calculated scaling functions to the peculiarities of the NMDs in different regions of momenta. It is concluded that the existing data on ψ' and y scaling are informative for NMDs at momenta not larger than 2.0–2.5 fm^{-1}. The CDFM allows us to study simultaneously and on the same footing the role of both basic quantities—the momentum and density distributions—for the description of scaling and superscaling phenomena in nuclei.

DOI: 10.1103/PhysRevC.71.014317 PACS number(s): 25.30.Fj, 21.60.−n, 21.10.Ft, 24.10.Jv

I. INTRODUCTION

The inclusive scattering of electrons as weakly interacting probes from the constituents of a composite nuclear system is a strong tool for gaining information about nuclear structure, particularly with regard to such basic quantities of the nuclear ground state as the local density and the momentum distributions of the nucleons. As we know [1,2] (see also [3–5]), the mean-field approximation (MFA) is unable to describe simultaneously these two important nuclear characteristics. Therefore, a consistent analysis of the role of nucleon-nucleon correlations is required using theoretical methods beyond the MFA in the description of the results of relevant experiments. It was realized that the nucleon momentum distribution (NMD), $n(k)$, which is related to both diagonal and nondiagonal elements of the one-body density matrix, is much more sensitive to the nucleon correlation effects than is the density distribution $\rho(r)$, which is given by its diagonal elements. Thus it is important to study these two basic characteristics simultaneously and consistently within the framework of a given theoretical correlation method analyzing the existing empirical data. Such a possibility appears in the coherent density fluctuation model (CDFM) [4–8], which is related to the δ-function limit of the generator coordinate method (see also [9]). The main aim of the present work is to apply the CDFM to the description of experimental data on the inclusive electron scattering from nuclei, which showed scaling and superscaling behavior of properly defined scaling functions, and to gain more information on the NMD and the density distributions in nuclei.

In the beginning of Sec. II we will review briefly scaling of both the first and second kind. Scaling of the first kind means that in the asymptotic regime of large transfer momenta $q = |\mathbf{q}|$ and energy ω a properly defined function of both of them $F(q, \omega)$ (which is generally the ratio between the inclusive cross section and the single-nucleon electromagnetic cross section) becomes a function only of a single variable, e.g., $y = y(q, \omega)$. This is called y scaling (see, e.g., [10–18]). Indeed, for the region $y < 0$ and $q > 500$ MeV/c this scaling is quite well obeyed. It has been found that the scaling function is related to the NMD, and thus some information (though model-dependent) can be obtained from the y-scaling analysis. Another scaling variable ψ' (related to y) and the corresponding ψ'-scaling function $f(\psi')$ have been defined and considered (see, e.g., [19–22]) within the framework of the relativistic Fermi gas (RFG) model. Studies of inclusive scattering cross section data found that $f(\psi')$ shows for $\psi' < 0$ both scaling of the first kind (independence of q) and scaling of the second kind (independence of the mass number A for a wide range of nuclei from ^{4}He to ^{197}Au). This is the so-called superscaling phenomenon [19]. The extension of the ψ'-scaling studies using the RFG model was given in [23,24]. Here we would like to emphasize that, as pointed out in [21], the actual nuclear dynamical content of superscaling is more complex than that provided by the RFG model. For instance, the superscaling behavior of the experimental data for $f(\psi')$ has been observed for large negative values of ψ' (up to $\psi' \approx -2$), while in the RFG model $f(\psi') = 0$ for $\psi' \leqslant -1$. This demonstrated the need to consider superscaling in theoretical approaches that go beyond the RFG model, i.e., for realistic finite nuclear systems. Such work was performed using the CDFM in [9]. The calculations in the model showed a good quantitative description of superscaling in finite nuclei for negative values of ψ', including those smaller than -1. We would like to note that the main ingredient of the CDFM (the weight function) was expressed and calculated in [9] on the

basis of experimentally known charge density distributions $\rho(r)$ for the ^{4}He, ^{12}C, ^{27}Al, ^{56}Fe, and ^{197}Au nuclei. At the same time, however, we started in [9] the discussion about the relation of $f(\psi')$ with the NMD, $n(k)$, showing implicitly how $f(\psi')$ can be calculated on the basis of $n(k)$. In Ref. [9] we indicated an alternative path for defining the weight function of the CDFM, which is built up from a phenomenological or a theoretical momentum distribution. In the present paper we give (in Sec. II) and use (in Sec. III) the explicit relationship of $f(\psi')$ with $n(k)$ using the basic scheme of the CDFM and showing also how information about $n(k)$ can be extracted from the ψ'-scaling function. We point out in our theoretical scheme and in our calculations the equivalence of cases when $f(\psi')$ is expressed through both density $\rho(r)$ and momentum distribution $n(k)$. In this way both basic quantities are used and can be analyzed simultaneously in studies of the scaling phenomenon.

To add to the work in [9], we present calculations of $f(\psi')$ for $q = 1560$ MeV/c and compare the results with the experimental data from [22]. We also define the y-scaling function $F(y)$ in the CDFM (Sec. II) and present the comparison with the experimental data (taken from [13,14]) of our calculations of $F(y)$ based on three different NMDs: from the CDFM, from the y-scaling (YS) studies in [13,14], and from the parameter-free theoretical approach based on the light-front dynamics (LFD) method [25] (Sec. III). We discuss the sensitivity of the calculated function $F(y)$ to the peculiarities of the different NMDs considered.

We also estimate the relationship of $f(\psi')$ with $F(y)$ and show in Sec. III the condition under which the NMD $n_{\rm CW}(k)$ extracted from the YS analyses [13,14] can describe the empirical data on $f(\psi')$.

The consideration of the points mentioned above made it possible to estimate approximately the region of momenta in $n(k)$ that is mainly responsible for the description of y and ψ' scaling and how it is related to the experimentally studied regions of the scaling variables y and ψ'. The conclusions of the present work are summarized in Sec. IV.

II. THE THEORETICAL SCHEME

We start this section with a brief review of the y- and ψ'-scaling analyses in Secs. II A and II B, respectively. An important point that we emphasize is the way in which the excitation of the residual system is taken into account, which is different in each case. We discuss the peculiarities of both approaches that are necessary to account for the development performed in our work within the CDFM (Secs. II C and II D).

A. Brief review of the *y* scaling

In this section we outline the main relationships concerning y scaling in the inclusive electron scattering of high-energy electrons from nuclei (e.g., [10–17]). At large transfer momentum ($q > 500$ MeV/c) and transfer energy ω, the scaling function $F(q,\omega)$, which is the cross section of the inclusive process divided by the elementary probe-constituent cross section, turns out to be a function of only a single variable $y = y(q,\omega)$. This is the scaling of the first kind. The smallest value of the missing momentum $p = |\mathbf{p}| = |\mathbf{p}_N - \mathbf{q}|$ ($\mathbf{p}_N$ being the momentum of the outgoing nucleon) at the smallest value of the missing energy is defined to be y ($-y$) for ω larger (smaller) than its value at the quasielastic peak

$$\omega \simeq \left(q^2 + m_N^2\right)^{1/2} - m_N, \tag{1}$$

m_N being the nucleon mass. The condition for the smallest missing energy means that the value of the quantity

$$\mathcal{E}(p) = \sqrt{(M_{A-1})^2 + p^2} - \sqrt{\left(M^0_{A-1}\right)^2 + p^2}, \tag{2}$$

where M_{A-1} is generally the excited recoiling system's mass and M^0_{A-1} is the mass of the system in its ground state, must be

$$\mathcal{E}(p) = 0. \tag{3}$$

The quantity $\mathcal{E}(p)$ in (2) characterizes the degree of excitation of the residual system, and essentially it is the missing energy (E_m) minus the separation energy (E_s). So, at condition (3) $E_m = E_s$.

As shown, e.g., in [11–14], for $q > 500$ MeV/c,

$$F(q,y) \stackrel{q\to\infty}{\longrightarrow} F(y) = f(y) - B(y), \tag{4}$$

where

$$f(y) = 2\pi \int_{|y|}^{\infty} n(k) k dk, \tag{5}$$

and $n(k)$ is the conventional NMD function normalized to unity

$$\int d\mathbf{k} n(\mathbf{k}) = 1. \tag{6}$$

The information on $F(y)$ and, correspondingly, on $f(y)$ can be used to obtain $n(k)$ by

$$n(k) = -\frac{1}{2\pi y}\frac{df(y)}{dy}\bigg|_{|y|=k}. \tag{7}$$

In Eq. (4), $B(y)$ is the binding correction, which is related to the part of the spectral function generated by ground-state correlations and the excitations of the residual system [when $M_{A-1} > M^0_{A-1}$ and, correspondingly, $\mathcal{E}(p) > 0$].

The problem of correctly accounting for the binding correction is a long-standing one. Only when the excitation energy of the residual system is equal to zero (as in the case of the deuteron) $B = 0$ and then $F(y) = f(y)$. Generally, however, the final system of $A-1$ nucleons can be left in all possible excited states. Then $B(y) \neq 0$ and $F(y) \neq f(y)$.

In [13] a new y-scaling variable ($y_{\rm CW}$) was introduced on the basis of a realistic nuclear spectral function as provided by few- and many-body calculations [26,27]. The use of $y_{\rm CW}$ leads to $B(y_{\rm CW}) = 0$ and, consequently, to $F(y_{\rm CW}) = f(y_{\rm CW})$. The latter is important because in this case it becomes possible to obtain information on the NMD directly [using Eq. (7)] without introducing the theoretical binding correction $B(y)$. In this consideration the removal energy (whose effects are a source of scaling violation, the other source being the final-state interactions) is taken into account in the definition of the scaling variable. So, the binding corrections are incorporated into the definition of $y_{\rm CW}$.

The analysis of empirical data on inclusive electron scattering from nuclei (with $A \leqslant 56$) showed [13,14] that the following form of $f(y)$ gives a very good agreement with the data:

$$f(y) = \frac{C_1 \exp(-a^2 y^2)}{\alpha^2 + y^2} + C_2 \exp(-b|y|)\left(1 + \frac{by}{1 + y^2/\alpha^2}\right), \tag{8}$$

where the first term describes the small y behavior and the second term dominates large y. From Eq. (7) one can obtain

$$n(k) = n_{\mathrm{MFA}}(k) + n_{\mathrm{corr}}(k), \tag{9}$$

where the mean-field part $n_{\mathrm{MFA}}(k)$ of the NMD (for $k \lesssim 2\ \mathrm{fm}^{-1}$) is

$$n_{\mathrm{MFA}}(k) = \frac{C_1}{\pi}[1 + a^2(\alpha^2 + k^2)]\frac{\exp(-a^2k^2)}{(\alpha^2 + k^2)^2}, \tag{10}$$

while the high-momentum components of $n(k)$ which contain nucleon correlation effects are given by

$$n_{\mathrm{corr}}(k) = \frac{C_2 b \exp(-bk)}{2\pi(1 + k^2/\alpha^2)}\left[b + \frac{k}{\alpha^2}\left(3 + bk + \frac{k^2}{\alpha^2}\right)\right]. \tag{11}$$

Later in our work we will use the information about $n(k)$ from the y-scaling analysis [Eqs. (9)–(11)]. The values of the parameters [13,14], e.g., in the case of interest for the ^{56}Fe nucleus, are $b = 1.1838$ fm, $C_1 = 0.30\ \mathrm{fm}^{-1}$, $C_2 = 0.11838$ fm, $\alpha = 0.710\ \mathrm{fm}^{-1}$, and $a = 0.908$ fm.

B. The ψ'-scaling variable and the ψ'-scaling function in the relativistic Fermi gas model and the relation between the y- and ψ'-scaling variables

In this section we briefly review scaling in the framework of the RFG model [19–22]. This is necessary for our consideration of scaling in the present work within the CDFM in Sec. II C and II D. The y-scaling variable in the RFG has the form

$$y_{\mathrm{RFG}} = m_N\left(\lambda\sqrt{1 + \frac{1}{\tau}} - \kappa\right), \tag{12}$$

where

$$\kappa \equiv q/2m_N, \quad \lambda \equiv \omega/2m_N, \quad \tau \equiv |Q^2|/4m_N^2 = \kappa^2 - \lambda^2 \tag{13}$$

are the dimensionless versions of q, ω and the squared four-momentum $|Q^2|$. In [19–22] a new scaling variable ψ was introduced by

$$\psi = \frac{1}{\sqrt{\xi_F}}\frac{\lambda - \tau}{\sqrt{(1 + \lambda)\tau + \kappa\sqrt{\tau(1 + \tau)}}}, \tag{14}$$

where

$$\xi_F = \sqrt{1 + \eta_F^2} - 1 \quad \text{and} \quad \eta_F = k_F/m \tag{15}$$

are the dimensionless Fermi kinetic energy and Fermi momentum, respectively.

To include, at least partially, the missing energy dependence in the scaling variable, a shift of the energy ω is introduced in the RFG [21] as

$$\omega' \equiv \omega - E_{\mathrm{shift}}, \tag{16}$$

where E_{shift} is chosen empirically (in practice it is from 15 to 25 MeV) and thus can take values other than the separation energy E_s. The corresponding λ and τ become

$$\lambda' \equiv \omega'/2m_N, \quad \tau' \equiv \kappa^2 - \lambda'^2. \tag{17}$$

This procedure aims to account for the effects of both binding in the initial state and interaction strength in the final state. It is shown in [21] that the corresponding new version of the ψ-scaling variable (ψ') has the following relation to the y-scaling variable:

$$\begin{aligned}\psi' \equiv \psi[\lambda \to \lambda'] = \frac{y_\infty(\widetilde{\lambda} = \lambda')}{k_F}\Bigg(1 + \sqrt{1 + \frac{1}{4\kappa^2}}\frac{1}{2}\,\eta_F \\ \times \frac{y_\infty(\widetilde{\lambda} = \lambda')}{k_F}\Bigg) + \mathcal{O}\big[\eta_F^2\big], \\ \widetilde{\lambda} \equiv \frac{\widetilde{\omega}}{2m_N} = \frac{\omega - E_s}{2m_N}.\end{aligned} \tag{18}$$

In (18) y_∞ is the y-scaling variable in the limit where $M^0_{A-1} \longrightarrow \infty$. k_F is the Fermi momentum, which is a free parameter in the RFG model, taking values from 1.115 fm^{-1} for ^{12}C to 1.216 fm^{-1} for ^{197}Au [21]. As shown in [21], Eq. (18) contains an important average dependence on the quantity $\mathcal{E}(p)$ in (2) (i.e., on the missing energy) which is reflected in the quadratic dependence of ψ' on the y-scaling variable.

Finally, in [21,22] a dimensionless scaling function is introduced within the RFG model

$$f_{\mathrm{RFG}}(\psi') = k_F F_{\mathrm{RFG}}(\psi'). \tag{19}$$

The careful analysis of the experimental data on inclusive electron scattering [21,22] shows not only that the RFG model contains scaling of the first kind (f or F are not dependent on q at high-momentum transfer and depend only on ψ') but also that $f(\psi')$ is independent of k_F to leading order in η_F^2, thus showing no dependence on the mass number A (scaling of the second kind). In the RFG, both kinds of scaling occur and this phenomenon is called superscaling.

The analytical form of f_{RFG} obtained in [19–22] which will be used in this work is

$$\begin{aligned}f_{\mathrm{RFG}}(\psi') = \frac{3}{4}(1 - \psi'^2)\Theta(1 - \psi'^2)\frac{1}{\eta_F^2} \\ \times \big[\eta_F^2 + \psi'^2\big(2 + \eta_F^2 - 2\sqrt{1 + \eta_F^2}\big)\big].\end{aligned} \tag{20}$$

Note that due to the Θ function in (20), the function $f(\psi')$ is equal to zero at $\psi' \leqslant -1$ and $\psi' \geqslant 1$. As can be seen in Fig. 1 of Ref. [9], this is not in accordance with the experimental data and justifies the attempt made in [9], as well as the development made in the present work, to consider superscaling in realistic systems beyond the RFG model.

C. Theoretical scheme of the CDFM and the ψ'-scaling function in the model

The CDFM suggested and developed in [4–8] was deduced from the δ-function limit of the generator coordinate method [28]. The model was applied to the study of the superscaling phenomenon in [9]. We now continue the development of the model, aiming its applications to the studies of the NMD from the analyses of y and ψ' scaling in inclusive electron scattering from nuclei. We start with the expressions of the Wigner distribution function (WDF) in the CDFM $W(\mathbf{r}, \mathbf{p})$ (e.g., [4,5]). They are based on two representations of the WDF for a piece of nuclear matter that contains all A nucleons distributed homogeneously in a sphere with radius R, with density

$$\rho_0(R) = \frac{3A}{4\pi R^3}, \tag{21}$$

and Fermi momentum

$$\overline{k}_F = k_F(R) = \left(\frac{3\pi^2}{2}\rho_0(R)\right)^{1/3} \equiv \frac{\alpha}{R},$$
$$\alpha = \left(\frac{9\pi A}{8}\right)^{1/3} \simeq 1.52A^{1/3}. \tag{22}$$

The first form of the WDF is

$$W_R(\mathbf{r}, \mathbf{p}) = \frac{4}{(2\pi)^3}\Theta(R - |\mathbf{r}|)\Theta(k_F(R) - |\mathbf{p}|). \tag{23}$$

The second form of the WDF for such a piece of nuclear matter can be written as

$$W_{\overline{k}_F}(\mathbf{r}, \mathbf{p}) = \frac{4}{(2\pi)^3}\Theta(\overline{k}_F - |\mathbf{p}|)\Theta\left(\frac{\alpha}{\overline{k}_F} - |\mathbf{p}|\right). \tag{24}$$

In the CDFM, the WDF, as well as the corresponding one-body density matrix (ODM), can be written as superpositions of WDFs (ODMs) from Eqs. (23) and (24) in coordinate and momentum space, respectively,

$$W(\mathbf{r}, \mathbf{p}) = \int_0^\infty dR|F(R)|^2 W_R(\mathbf{r}, \mathbf{p})$$
$$= \frac{4}{(2\pi)^3}\int_0^\infty dR|F(R)|^2\Theta(R - |\mathbf{r}|)\Theta(k_F(R) - |\mathbf{p}|) \tag{25}$$

and

$$W(\mathbf{r}, \mathbf{p}) = \int_0^\infty d\overline{k}_F|G(\overline{k}_F)|^2 W_{\overline{k}_F}(\mathbf{r}, \mathbf{p})$$
$$= \frac{4}{(2\pi)^3}\int_0^\infty d\overline{k}_F|G(\overline{k}_F)|^2\Theta(\overline{k}_F - |\mathbf{p}|)\Theta\left(\frac{\alpha}{\overline{k}_F} - |\mathbf{r}|\right). \tag{26}$$

The relationship between both $|F|^2$ and $|G|^2$ functions is

$$|G(\overline{k}_F)|^2 = \frac{\alpha}{\overline{k}_F{}^2}\left|F\left(\frac{\alpha}{\overline{k}_F}\right)\right|^2. \tag{27}$$

Using the basic relationships of the density and momentum distributions with the WDF,

$$\rho(\mathbf{r}) = \int d\mathbf{p}W(\mathbf{r}, \mathbf{p}), \tag{28}$$

$$n(\mathbf{p}) = \int d\mathbf{r}W(\mathbf{r}, \mathbf{p}), \tag{29}$$

one can obtain the corresponding expressions for $\rho(r)$ and $n(p)$ using the WDF from Eq. (25), that is,

$$\rho(\mathbf{r}) = \int_0^\infty dR|F(R)|^2\frac{3A}{4\pi R^3}\Theta(R - |\mathbf{r}|), \tag{30}$$

$$n(\mathbf{p}) = \frac{2}{3\pi^2}\int_0^{\alpha/p} dR|F(R)|^2 R^3. \tag{31}$$

Equivalently, using the WDF from Eq. (26), one obtains

$$\rho(\mathbf{r}) = \frac{2}{3\pi^2}\int_0^\infty d\overline{k}_F|G(\overline{k}_F)|^2\Theta\left(\frac{\alpha}{r} - \overline{k}_F\right)\overline{k}_F{}^3, \tag{32}$$

$$n(\mathbf{p}) = \int_0^\infty d\overline{k}_F|G(\overline{k}_F)|^2\frac{3A}{4\pi\overline{k}_F{}^3}\Theta(\overline{k}_F - |\mathbf{p}|). \tag{33}$$

Both are normalized to the mass number

$$\int \rho(\mathbf{r})d\mathbf{r} = A, \quad \int n(\mathbf{k})d\mathbf{k} = A \tag{34}$$

when both weight functions are normalized to unity

$$\int_0^\infty dR|F(R)|^2 = 1, \quad \int_0^\infty d\overline{k}_F|G(\overline{k}_F)|^2 = 1. \tag{35}$$

One can see from Eqs. (30), (31) and (32), (33) the symmetry of the expressions for $\rho(r)$ and $n(p)$ as integrals in the coordinate and momentum space.

A convenient approach to obtaining the weight functions $F(R)$ and $G(\overline{k}_F)$ is to use a known (experimental or theoretical) density distribution $\rho(r)$ and/or the momentum distribution $n(p)$ for a given nucleus. For $|F(R)|^2$ one can obtain from Eqs. (30) and (31)

$$|F(R)|^2 = -\frac{1}{\rho_0(R)}\left.\frac{d\rho(r)}{dr}\right|_{r=R} \tag{36}$$

at $d\rho/dr \leqslant 0$, and

$$|F(R)|^2 = -\frac{3\pi^2}{2}\frac{\alpha}{R^5}\left.\frac{dn(p)}{dp}\right|_{p=\alpha/R} \tag{37}$$

at $dn/dp \leqslant 0$.

The expressions for $|G(\overline{k}_F)|^2$ can be obtained from Eqs. (32) and (33) as

$$|G(\overline{k}_F)|^2 = -\frac{3\pi^2}{2}\frac{\alpha}{\overline{k}_F{}^5}\left.\frac{d\rho(r)}{dr}\right|_{r=\alpha/\overline{k}_F} \tag{38}$$

at $d\rho/dr \leqslant 0$, and

$$|G(\overline{k}_F)|^2 = -\frac{1}{n_0(\overline{k}_F)}\left.\frac{dn(p)}{dp}\right|_{p=\overline{k}_F} \tag{39}$$

at $dn/dp \leqslant 0$, with

$$n_0(\overline{k}_F) = \frac{3A}{4\pi\overline{k}_F{}^3}. \tag{40}$$

To introduce the scaling function within the CDFM, we assume that the scaling function for a finite nucleus $f(\psi')$ can be defined and obtained by means of the weight

function $|F(R)|^2$ (and $|G(\overline{k}_F)|^2$) weighting the scaling function for the RFG model depending on the scaling variable ψ'_R [$f_{\rm RFG}(\psi' = \psi'_R)$, Eq. (20)], corresponding to a given density $\rho_0(R)$ from (21) and Fermi momentum $k_F(R)$ from (22) [9] [or corresponding to a given density in the momentum space $n_0(\overline{k}_F)$ as in (40)].

One can write the scaling variable ψ'_R in the form [9]

$$\psi'_R(y) = \frac{p(y)}{k_F(R)} = \frac{p(y)R}{\alpha}, \tag{41}$$

where

$$p(y) = \begin{cases} y(1+cy), & y \geqslant 0 \\ -|y|(1-c|y|), & y \leqslant 0,\ |y| \leqslant 1/2c \end{cases} \tag{42}$$

with

$$c \equiv \frac{1}{2m_N}\sqrt{1+\frac{1}{4\kappa^2}}. \tag{43}$$

Also a more convenient notation can be used:

$$\psi'_R(y) = \frac{k_F}{k_F(R)}\frac{p(y)}{k_F} = \frac{k_F}{k_F(R)}\psi'. \tag{44}$$

Using the Θ function in Eq. (20), one can define the scaling function for a finite nucleus by the following expressions:

$$f(\psi') = \int_0^{\alpha/(k_F|\psi'|)} dR|F(R)|^2 f_{\rm RFG}(R,\psi'), \tag{45}$$

with

$$\begin{aligned} f_{\rm RFG}(R,\psi') = \frac{3}{4}\left[1-\left(\frac{k_F R|\psi'|}{\alpha}\right)^2\right]\Bigg\{1+\left(\frac{Rm_N}{\alpha}\right)^2 \\ \times\left(\frac{k_F R|\psi'|}{\alpha}\right)^2\Bigg[2+\left(\frac{\alpha}{Rm_N}\right)^2 \\ -2\sqrt{1+\left(\frac{\alpha}{Rm_N}\right)^2}\Bigg]\Bigg\}, \end{aligned} \tag{46}$$

and equivalently by

$$f(\psi') = \int_{k_F|\psi'|}^{\infty} d\overline{k}_F|G(\overline{k}_F)|^2 f_{\rm RFG}(\overline{k}_F,\psi'), \tag{47}$$

with

$$\begin{aligned} f_{\rm RFG}(\overline{k}_F,\psi') = \frac{3}{4}\left[1-\left(\frac{k_F|\psi'|}{\overline{k}_F}\right)^2\right] \\ \times\left\{1+\left(\frac{m_N}{\overline{k}_F}\right)^2\left(\frac{k_F|\psi'|}{\overline{k}_F}\right)^2\right. \\ \left.\times\left[2+\left(\frac{\overline{k}_F}{m_N}\right)^2-2\sqrt{1+\left(\frac{\overline{k}_F}{m_N}\right)^2}\right]\right\}. \end{aligned} \tag{48}$$

In this way in the CDFM the scaling function $f(\psi')$ is an infinite superposition of the RFG scaling functions $f_{\rm RFG}(R,\psi')$ [or $f_{\rm RFG}(\overline{k}_F,\psi')$].

In Eqs. (45)–(48) the momentum k_F is not a free fitting parameter for different nuclei, as in the RFG model, but it can be calculated consistently in the CDFM for each nucleus [see (36)–(39)] using the expression

$$\begin{aligned} k_F &= \int_0^\infty dRk_F(R)|F(R)|^2 \\ &= \alpha\int_0^\infty dR\frac{1}{R}|F(R)|^2 \\ &= \frac{4\pi(9\pi)^{1/3}}{3A^{2/3}}\int_0^\infty dR\rho(R)R, \end{aligned} \tag{49}$$

when the condition

$$\lim_{R\to\infty}[\rho(R)R^2] = 0 \tag{50}$$

is fulfilled and, equivalently,

$$k_F = \frac{16\pi}{3A}\int_0^\infty d\overline{k}_F n(\overline{k}_F)\overline{k}_F{}^3, \tag{51}$$

when the condition

$$\lim_{\overline{k}_F\to\infty}[n(\overline{k}_F)\overline{k}_F{}^4] = 0 \tag{52}$$

is fulfilled. Generally, Eqs. (50) and (52) are fulfilled, so Eqs. (49) and (51) can be used to calculate k_F in most cases.

The integration in (45) and (47), using Eqs. (36)–(39), leads to the following expressions for $f(\psi')$:

$$\begin{aligned} f(\psi') = \frac{4\pi}{A}\int_0^{\alpha/(k_F|\psi'|)} dR\rho(R)\Bigg[R^2 f_{\rm RFG}(R,\psi') \\ +\frac{R^3}{3}\frac{\partial f_{\rm RFG}(R,\psi')}{\partial R}\Bigg] \end{aligned} \tag{53}$$

and

$$\begin{aligned} f(\psi') = \frac{4\pi}{A}\int_{k_F|\psi'|}^\infty d\overline{k}_F n(\overline{k}_F)\Bigg[\overline{k}_F{}^2 f_{\rm RFG}(\overline{k}_F,\psi') \\ +\frac{\overline{k}_F{}^3}{3}\frac{\partial f_{\rm RFG}(\overline{k}_F,\psi')}{\partial\overline{k}_F}\Bigg], \end{aligned} \tag{54}$$

the latter at

$$\lim_{\overline{k}_F\to\infty}[n(\overline{k}_F)\overline{k}_F{}^3] = 0, \tag{55}$$

where the functions $f_{\rm RFG}(R,\psi')$ and $f_{\rm RFG}(\overline{k}_F,\psi')$ are given by Eqs. (46) and (48), respectively. We emphasize the symmetry in both Eqs. (53) and (54). We also note that the CDFM scaling function $f(\psi')$ is symmetric at the change of ψ' to $-\psi'$.

The scaling function $f(\psi')$ can be calculated using Eqs. (53) and (54) by means of (i) its relationship to the density distribution $\rho(r)$ and (ii) from the relationship to the NMD $n(p)$. Both quantities (ρ and n) can be taken from empirical data or from theoretical calculations. In the CDFM they are consistently related because they are based on the WDF of the model [Eqs. (25) and (26)]. Using experimentally known density distributions $\rho(r)$ for a given nucleus, one can calculate the weight functions $|F|^2$ [Eq. (36)] or $|G|^2$ [Eq. (38)] and by means of them, calculate $n(p)$ in the CDFM [by Eqs. (31) or (33), respectively].

From Eq. (54) one can estimate the possibility to obtain information about the NMD from the empirical data on the scaling function $f(\psi')$. If we keep only the main term of the function

$$f_{\rm RFG}(\overline{k}_F, \psi') \simeq \frac{3}{4}\left(1 - \frac{(k_F|\psi'|)^2}{\overline{k}_F{}^2}\right) \tag{56}$$

and its derivative

$$\frac{\partial f_{\rm RFG}(\overline{k}_F, \psi')}{\partial \overline{k}_F} \simeq \frac{3}{2}\frac{(k_F|\psi'|)^2}{\overline{k}_F{}^3}, \tag{57}$$

then

$$f(\psi') \simeq 3\pi \int_{k_F|\psi'|}^{\infty} d\overline{k}_F n(\overline{k}_F)\overline{k}_F{}^2\left[1 - \frac{1}{3}\frac{(k_F|\psi'|)^2}{\overline{k}_F{}^2}\right]. \tag{58}$$

In Eq. (58)

$$\int n(\overline{\mathbf{k}}_F)d\overline{\mathbf{k}}_F = 1. \tag{59}$$

Neglecting the second term in the bracket in (58) [because $\frac{1}{3}\frac{(k_F|\psi'|)^2}{\overline{k}_F{}^2} \ll 1$] one obtains

$$f(\psi') \simeq 3\pi \int_{k_F|\psi'|}^{\infty} d\overline{k}_F n(\overline{k}_F)\overline{k}_F{}^2. \tag{60}$$

Taking the derivative on $|\psi'|$ from both sides of Eq. (60) leads to

$$n(p) = -\left.\frac{1}{3\pi p^2 k_F}\frac{\partial f(\psi')}{\partial(|\psi'|)}\right|_{|\psi'|=p/k_F}. \tag{61}$$

Eq. (61) can give approximate information on the NMD $n(p)$. If one keeps the second term in the bracket under the integral in (58), then a more complicated equation results:

$$\left.\frac{\partial f(\psi')}{\partial(k_F|\psi'|)}\right|_{k_F|\psi'|=p} = -2\pi p^2 n(p) - 2\pi p\int_p^{\infty} dk' n(k'). \tag{62}$$

D. *y*-scaling function in the CDFM and the relationship between the *y*- and ψ'-scaling functions in the model

To define the y-scaling function $F(y)$ (with dimensions) in the CDFM and to establish the relationship between the latter and the dimensionless scaling function $f(\psi')$ [Eqs. (53) and (54)] we start with the expression that relates both functions in the RFG model [21,22]:

$$F_{\rm RFG}(y) = \frac{f_{\rm RFG}(\overline{k}_F, \psi'(y))}{\overline{k}_F}. \tag{63}$$

Analogous to the definition of $f(\psi')$ in the CDFM, we introduce the function $F(y)$ in a finite system as a superposition of RFG y-scaling functions $F_{\rm RFG}(y)$ (63) such that

$$F(y) = \int_{k_F|\psi'|=|p(y)|}^{\infty} d\overline{k}_F |G(\overline{k}_F)|^2 \frac{f_{\rm RFG}(k_F|\psi'| = |p(y)|, \overline{k}_F)}{\overline{k}_F}, \tag{64}$$

where the function $f_{\rm RFG}$ has the form (48) and $k_F|\psi'| = |p(y)|$ with $p(y)$ given by Eq. (42). Using Eq. (39) for $|G(\overline{k}_F)|^2$, we obtain from Eq. (64)

$$F(y) = \frac{4\pi}{3}\int_{k_F|\psi'|=|p(y)|}^{\infty} d\overline{k}_F n(\overline{k}_F)\left\{2k f_{\rm RFG}(|p(y)|, \overline{k}_F) + \overline{k}_F{}^2\frac{\partial f_{\rm RFG}(|p(y)|, \overline{k}_F)}{\partial \overline{k}_F}\right\}. \tag{65}$$

Keeping in Eq. (65) the main terms of the function $f_{\rm RFG}$ [Eq. (56)] and of its derivative $\partial f_{\rm RFG}/\partial \overline{k}_F$ [Eq. (57)], one obtains the scaling function

$$F(y) \simeq 2\pi \int_{|p(y)|}^{\infty} dk\, k n(k). \tag{66}$$

In Eqs. (65) and (66) the normalization of $n(k)$ is

$$\int n(\mathbf{k})d\mathbf{k} = 1. \tag{67}$$

For the cases of interest when $y \leqslant 0$ and $|y| \leqslant 1/(2c)$,

$$F(y) \simeq 2\pi \int_{|y|(1-c|y|)}^{\infty} dk\, k n(k). \tag{68}$$

If the ψ'-scaling variable is not a quadratic function of y as in [21,22] [see Eq. (18)] but is a linear one (i.e., $k_F|\psi'| = |y|$), then

$$F(y) \simeq 2\pi \int_{|y|}^{\infty} dk\, k n(k). \tag{69}$$

Equation (69) gives the known y-scaling function [10–14] and its relationship with the NMD $n(k)$. It can be seen from (68) that the use of a more complicated (quadratic) dependence of ψ' on y [21,22] leads to a more complicated y-scaling function in the CDFM and its relationship with the NMD.

We end this section by elaborating somewhat more on Eq. (60), considering the relationship between the scaling variables y and ψ' and between the corresponding scaling functions. Equation (60) for the ψ'-scaling function $f(\psi')$ can be rewritten in the following approximate form:

$$f(\psi') \simeq 3\pi \int_{k_F|\psi'|}^{\infty} d\overline{k}_F n(\overline{k}_F)\overline{k}_F{}^2 \simeq \frac{3}{2}k_{\rm av} 2\pi \int_{k_F|\psi'|}^{\infty} d\overline{k}_F n(\overline{k}_F)\overline{k}_F. \tag{70}$$

If we admit as in the case of the y scaling [10–14] that

$$k_F|\psi'| = |y|, \tag{71}$$

then

$$f(\psi') = \tfrac{3}{2}k_{\rm av}F(y), \tag{72}$$

where $F(y)$ is the y-scaling function (69) and $k_{\rm av}$ can be estimated as in [13] to be

$$k_{\rm av} \simeq \left\langle\frac{1}{k}\right\rangle^{-1}, \qquad \text{where} \quad \left\langle\frac{1}{k}\right\rangle = \int d\mathbf{k}\frac{n(k)}{k}. \tag{73}$$

In the case of the ψ'-scaling variable (for $y \leqslant 0$),

$$k_F|\psi'| = |y|(1 - c|y|), \tag{74}$$

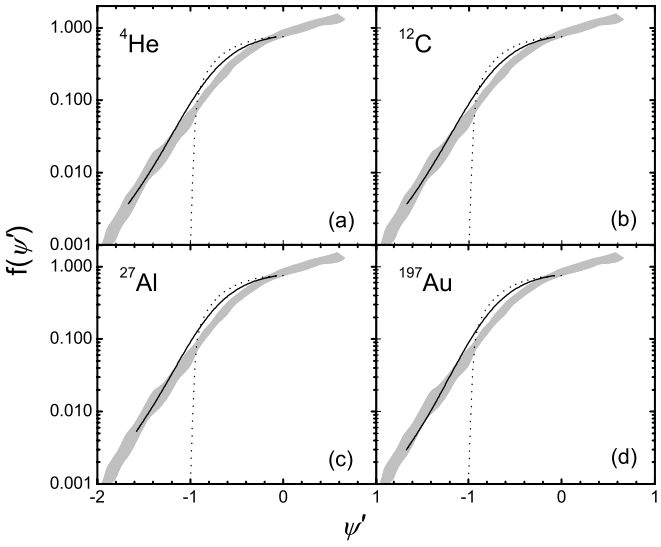

FIG. 1. Scaling function $f(\psi')$ in the CDFM (solid line) at $q = 1560$ MeV/c for ^{4}He, ^{12}C, ^{27}Al, and ^{197}Au. The results are obtained using Eqs. (53) and (49) and equivalently by Eqs. (54) and (51) with $n(p)$ from the CDFM [Eq. (31)]. The experimental data from [22] are given by the shaded area. The RFG result [Eq. (20)] is shown by the dotted line.

and we can replace approximately the lower limit of the integration by $|y|$ which is, however, the solution of Eq. (74), that is,

$$f(\psi') \simeq 3\pi \int_{|y|}^{\infty} d\overline{k}_F \, n(\overline{k}_F) \overline{k}_F{}^2,$$

$$\text{where} \quad |y| = \frac{1}{2c}\left(1 - \sqrt{1 - 4ck_F|\psi'|}\right). \tag{75}$$

III. RESULTS OF CALCULATIONS AND DISCUSSION

We begin this section with calculations of the scaling function $f(\psi')$ using Eqs. (53) and (54) for different nuclei within the CDFM for the transfer momentum $q = 1560$ MeV/c. The results for ^{4}He, ^{12}C, ^{27}Al, and ^{197}Au are presented in Fig. 1 and compared with the experimental data from [22] and with the predictions of the RFG model [Eq. (20)] with values of k_F from [21,22]. Our calculations are performed in addition to those for $q = 1000$ and 1650 MeV/c in [9] which were compared with the data from [21].

Following the main aim of our work, namely to extract reliable information on the NMD from the scaling function, we will consider in detail the consecutive steps of the calculations of $f(\psi')$ in connection with $n(k)$. We note first that $f(\psi')$ is calculated in the CDFM using Eq. (53) where the density distribution $\rho(r)$ is a Fermi-type with parameter values obtained from the experimental data on elastic electron scattering from nuclei and muonic atoms. For ^{4}He and ^{12}C we used a symmetrized Fermi-type density distribution [29] with the following half-radius $R_{1/2}$ and diffuseness b parameters: $R_{1/2} = 1.710$ fm, $b = 0.290$ fm for ^{4}He, and $R_{1/2} = 2.470$ fm, $b = 0.420$ fm for ^{12}C. These values of the parameters lead to charge rms radii equal to 1.710 fm for ^{4}He and 2.47 fm for ^{12}C, which coincide with the experimental ones [30]. For the ^{27}Al nucleus the values of $R_{1/2} = 3.070$ fm and $b = 0.519$ fm are taken from [30]. For ^{197}Au the parameter values are $R_{1/2} = 6.419$ fm [31] and $b = 1.0$ fm [9]. The necessity to use the latter value of b for ^{197}Au instead of $b = 0.449$ fm [31] was discussed in [9]. This *ad hoc* procedure was used to obtain high-momentum components of the NMD $n(k)$ [using (31) and (36)] similar to those in light and medium nuclei. This was necessary because of the particular A dependence of $n(k)$ in the CDFM resulting in lower tails of $n(k)$ at $k > 2$ fm^{-1} for the heaviest nuclei which has to be improved. Also for ^{56}Fe a better agreement with ψ'-scaling data at $q = 1000$ MeV/c is obtained for $b = 0.7$ fm instead of $b = 0.558$ fm [30]; this result will be shown later.

As can be seen, the CDFM results for the scaling function $f(\psi')$ agree well with the experimental data taken from inclusive electron scattering [22]. This is true even in the interval $\psi' < -1$ for all nuclei considered, in contrast to the results of the RFG model where $f_{\rm RFG}(\psi') = 0$ for $\psi' \leqslant -1$. Here we emphasize that our scaling function $f(\psi')$ is obtained using the experimental information on the density distribution. At the same time, however, $f(\psi')$ is related to the NMD $n(p)$, as can be seen from Eq. (54). We note that Eqs. (53) and (54) are equivalent when we calculate in the CDFM the NMD $n(p)$ consistently using Eq. (31), where the weight function $|F(R)|^2$ is calculated using the derivative of the density distribution $\rho(r)$ [Eq. (36)]. The same consistency exists in the calculations of the CDFM Fermi momentum k_F, which is used in the calculations of $f(\psi')$ from Eqs. (53) and (54). It is calculated by means of Eq. (49) and, equivalently, by Eq. (51) where the CDFM result for $n(p)$ is used. The calculated values of k_F in the CDFM are 1.201 fm^{-1} for ^{4}He, 1.200 fm^{-1} for ^{12}C, 1.267 fm^{-1} for ^{27}Al, and 1.270 and 1.200 fm^{-1} for ^{197}Au.

In Fig. 2 we give the results of the calculations of the NMD $n(k)$ within the CDFM for ^{4}He, ^{12}C, ^{27}Al, ^{56}Fe, and ^{197}Au using Eqs. (31), (36) and Fermi-density distribution ρ with the parameter values mentioned above (with $b = 1.0$ fm for ^{197}Au). The normalization is $\int n(\mathbf{k}) d\mathbf{k} = 1$. The $n(k)$ from CDFM for the nuclei considered are with similar tails at $k \gtrsim 1.5$ fm^{-1}, so they are combined and presented by a shaded area. As expected, this similarity of the high-momentum components of $n(k)$ leads to the superscaling phenomenon. In our work there is an explicit relation of the scaling function to the NMD in finite nuclear systems [Eq. (31)]. As can be seen, when the latter is calculated in a realistic nuclear model accounting for nucleon correlations beyond the MFA, a reasonable explanation of the superscaling behavior of the scaling function for $\psi' < -1$ is achieved.

In Fig. 2 we also give (i) the y-scaling data for $n(k)$ in ^{4}He, ^{12}C, and ^{56}Fe obtained from analyses of (e, e') cross sections in [12] on the basis of the y-scaling theoretical scheme; (ii) $n(k)$ calculated within the MFA using Woods-Saxon single-particle wave functions for ^{56}Fe; and (iii) the NMD for ^{56}Fe [Eq. (9)] extracted from the more recent y-scaling analyses in [13,14]. We also give the corresponding contributions to $n(k)$, namely the mean-field one $n_{\rm MFA}(k)$ [Eq. (10)] and the high-momentum component $n_{\rm corr}(k)$ [Eq. (11)], and (iv) the NMD $n(k)$, e.g., for

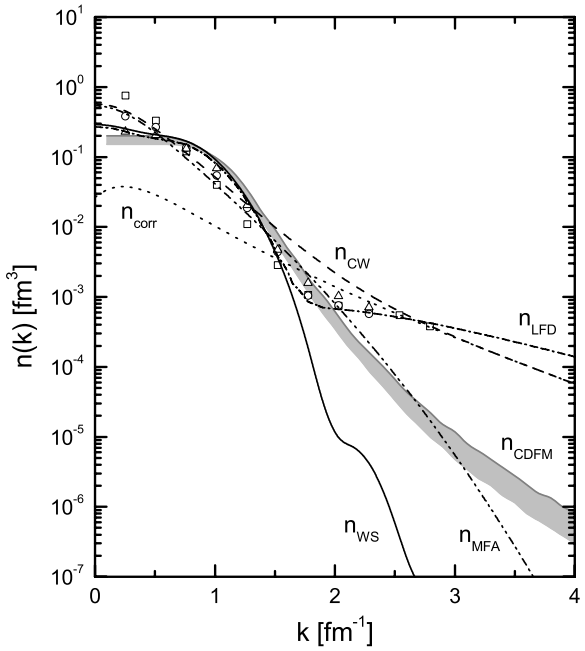

FIG. 2. Nucleon momentum distribution $n(k)$ from (i) CDFM: the calculated results using Eqs. (31) and (36) for ^{4}He, ^{12}C, ^{27}Al, ^{56}Fe, and ^{197}Au are combined by the shaded area ($n_{\rm CDFM}$); (ii) y-scaling data [12] given by open squares, circles, and triangles for ^{4}He, ^{12}C, and ^{56}Fe, respectively; (iii) $y_{\rm CW}$ analyses [13,14] for ^{56}Fe [Eq. (9)] ($n_{\rm CW}$), $n_{\rm MFA}$ [Eq. (10)], $n_{\rm corr}$ [Eq. (11)]; (iv) LFD approach [25] [Eqs. (76)–(79), (81), and (82)] for ^{56}Fe ($n_{\rm LFD}$); and (v) MFA calculations using Woods-Saxon single-particle wave functions for ^{56}Fe ($n_{\rm WS}$).

^{56}Fe obtained within an approach [25] based on the NMD in the deuteron from the light-front dynamics (LFD) method (e.g., [32,33] and references therein). In [25] $n(k)$ was written within the natural-orbital representation [34] as a sum of hole-state [$n^h(k)$] and particle-state [$n^p(k)$] contributions

$$n(k) = N_A[n^h(k) + n^p(k)]. \tag{76}$$

In (76)

$$n^h(k) = \sum_{nlj}^{\rm F.L.} 2(2j+1)\lambda_{nlj} C(k)|R_{nlj}(k)|^2, \tag{77}$$

where F.L. denotes the Fermi level, and

$$C(k) = \frac{m_N}{(2\pi)^3\sqrt{k^2+m_N^2}}. \tag{78}$$

In Eq. (77) λ_{nlj} are the natural occupation numbers (which for the hole states are close to unity and were set to be equal to unity in [25] with good approximation) and the hole-state natural orbitals $R_{nlj}(k)$ are replaced by single-particle wave functions from the MFA. In [25] Woods-Saxon single-particle wave functions were used for protons and neutrons. The use of other single-particle wave functions (e.g., from Hartree-Fock-Bogolyubov calculations) leads to similar results.

The normalization factor has the form

$$N_A = \left\{ 4\pi \int_0^\infty dq\, q^2 \times \left[\sum_{nlj}^{\rm F.L.} 2(2j+1)\lambda_{nlj} C(q)|R_{nlj}(q)|^2 + \frac{A}{2} n_5(q) \right] \right\}^{-1}. \tag{79}$$

In the following we use these well-known facts: (i) the high-momentum components of $n(k)$ caused by short-range and tensor correlations are almost completely determined by the contributions of the particle-state natural orbitals (e.g., [35]), and (ii) the high-momentum tails of $n(k)/A$ are approximately equal for all nuclei and are rescaled versions of the NMD in the deuteron $n_d(k)$ [36]:

$$n_A(k) \simeq \alpha_A n_d(k), \tag{80}$$

where α_A is a constant. These facts made it possible to assume in [25] that $n^p(k)$ is related to the high-momentum component $n_5(k)$ of the deuteron, that is,

$$n^p(k) = \frac{A}{2} n_5(k). \tag{81}$$

In (79) and (81), $n_5(k)$ is expressed by an angle-averaged function [25] as

$$n_5(k) = C(k)\overline{(1-z^2) f_5^2(k)}. \tag{82}$$

In Eq. (82) $z = \cos(\widehat{\mathbf{k}}, \widehat{\mathbf{n}})$, $\widehat{\mathbf{n}}$ being a unit vector along the three-vector ($\overrightarrow{\omega}$) component of the four-vector ω which determines the position of the light-front surface [32,33]. The function $f_5(k)$ is one of the six scalar functions $f_{1-6}(k^2, \mathbf{n}\cdot\mathbf{k})$ which are the components of the deuteron total wave function $\Psi(\mathbf{k}, \mathbf{n})$. The component f_5 exceeds sufficiently other f components for $k \geqslant 2$–2.5 fm^{-1} and is the main contribution to the high-momentum component of $n_d(k)$, incorporating the main part of the short-range features of the nucleon-nucleon interaction.

As can be seen in Fig. 2, the calculated LFD momentum distributions are in good agreement with the y-scaling data for ^{4}He, ^{12}C, and ^{56}Fe from [12], including the high-momentum region. We emphasize that $n(k)$ calculated in the LFD method contains no free parameters.

The comparison of the NMDs from the CDFM, LFD, and the y-scaling analysis (YS) [Eqs. (9)–(11)] shows their similarity for momenta $k \lesssim 1.5$ fm^{-1} (i.e., in the region where the MFA is a good approximation). It also shows their quite different decreasing slopes for $k > 1.5$ fm^{-1}, where the effects of nucleon correlations dominate. In the rest of this section we will consider in more detail the questions concerning the reliability of the NMD information obtained from the y- and ψ'-scaling analyses. These questions concern the sensitivity of such analyses and the identification of the intervals of momenta in which $n(k)$ can be obtained with more reliability from the experimental data and from the y- and ψ'-scaling studies. First of all, we emphasize that the approaches considered to obtain experimental information

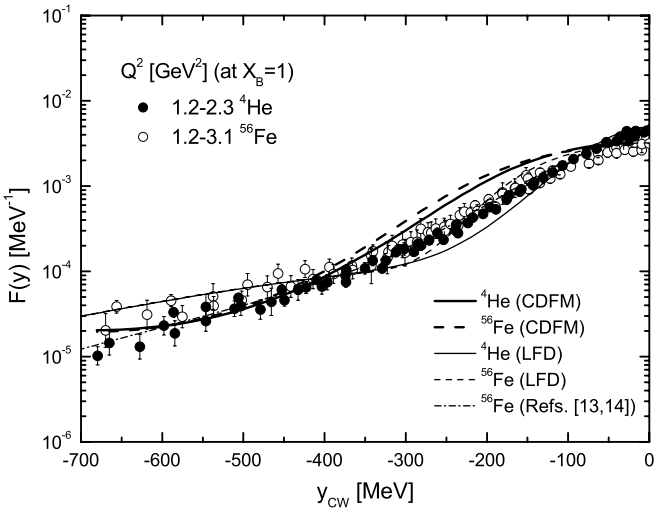

FIG. 3. The y-scaling function $F(y)$ for ^{4}He and ^{56}Fe calculated in the CDFM [Eq. (65)] (solid and thick dashed lines), from the $y_{\rm CW}$-scaling approach [13,14] [Eqs. (9)–(11)] for ^{56}Fe (dash-dotted line), and from the approach [25] within the LFD method [Eqs. (76)–(79), (81), and (82)] (thin solid and dashed lines). The results are compared with the $y_{\rm CW}$-scaling data taken from [13,14].

on $n(k)$ are strongly model dependent. In this respect we note various ways to introduce the scaling variables, e.g., the different y-scaling variables [12–14], the different ψ-scaling variables (e.g., in [19,21]), as well as the corresponding y- and ψ-scaling functions. Even so, it is worth considering in more detail the model-dependent empirical information about the NMD coming from y- and ψ-scaling analyses. We emphasize that our consideration is based on $f(\psi')$ and the y-scaling function $F(y)$ within the CDFM, as well as on the relationship between both of them discussed in Sec. II D.

First, we give the results of the calculations of the y-scaling function $F(y)$ obtained in the CDFM [Eq. (65)] using different NMD $n(k)$: (i) from the CDFM [Eqs. (31) and (36)], (ii) from the $y_{\rm CW}$-scaling approach [13,14] [Eqs. (9)–(11)], and (iii) from the approach [25] that uses the results of the LFD method [Eqs. (76)–(79), (81), and (82)]. In Fig. 3 they are compared with the $y_{\rm CW}$ scaling data for $F(y)$ for the ^{4}He and ^{56}Fe nuclei taken from [13,14]. As can be seen from Fig. 3, there is a general agreement with the data for all the NMDs considered. At first thought, this is surprising knowing the different behaviors of $n(k)$ for larger k as seen in Fig. 2. The reasons for the relative similarity of the results for $F(y)$ using different $n(k)$ are as follows.

The ψ'-scaling variable is a quadratic function of y but not a linear one [Eq. (18)]. In accordance with this, the lower limit of the integral [Eq. (65)] for $F(y)$ is not $|y|$ as in [13,14], but $|y|(1-c|y|)$ [see for a comparison Eqs. (68) and (69)]. Furthermore, because of the steep decreasing slope rates of the NMDs for large momenta, the main contribution to the integral (65) [and to the estimation (68)] comes from momenta that are not much larger than the lower limit of the integration. In this way, the very high-momentum components of $n(k)$ do not play so important a role [in the integral in (65)], at least for momenta studied so far at $y > -700$ MeV/c. Here are some numerical estimations: For example, for $y = -300$ MeV/c, instead of integrating from $|y| = 300$ MeV/$c = 1.52$ fm^{-1} [as in (69)], in $F(y)$ in (68) the integration starts from $|y|(1-c|y|) = 1.19$ fm^{-1}. For $y = -600$ MeV/c, instead of integrating from $|y| = 600$ MeV/$c = 3.04$ fm^{-1}, the lower limit of the integral in (68) is $|y|(1-c|y|) = 1.71$ fm^{-1}. This means that the main contribution to $F(y)$ from $n(k)$ is for momenta $k \lesssim 2$ fm^{-1}. The behavior of $F(y)$ in Fig. 3 reflects that contribution of $n(k)$. For instance, for $-400 \leqslant y \leqslant 0$ MeV/c the CDFM result for $F(y)$ is higher than those of LFD and YS because the values of $n(k)$ from CDFM for $k \leqslant 1.5$ fm^{-1} are larger than those of $n(k)$ from the LFD and the YS. In contrast to this, the values of $F(y)$ for $-700 \leqslant y \leqslant -400$ MeV/c in the CDFM result are lower than those of the LFD because $n(k)$ from LFD has a higher tail than $n(k)$ in the CDFM for $k > 1.5$ fm^{-1}. Nevertheless, though the tails of $n(k)$ for large k are quite different (for $k > 1.5$ fm^{-1}), the values of $F(y)$ from the different approaches are quite close to each other and in agreement with the existing data. In this way, we can conclude from our experience that the existing y-scaling data can give reliable information for the NMD for momenta not larger than 1.5–2.0 fm^{-1}, where the considered $n(k)$ are not drastically different from each other.

One can see from Fig. 3 that the CDFM results for $F(y)$ are in a very good agreement with the data for ^{4}He for $y \lesssim -400$ MeV/c, while in the same region the LFD result agrees very well with the data for ^{56}Fe. The YS result for $F(y)$ agrees well with the data for ^{56}Fe for $y \gtrsim -600$ MeV/c.

It is worth mentioning that in our approach we start from the ψ'-scaling consideration for the function $F(y)$ and this leads to a relatively good description of the y-scaling data on the basis of the correct accounting of the relationship between the ψ'- and y-scaling variables. The overall agreement of the theoretical results using the momentum distributions from the CDFM, LFD, and YS with the experimental data for $F(y)$ is related to their similarities up to momenta $k = 1.5$–2.0 fm^{-1}.

Our next step is to estimate the ψ'-scaling function $f(\psi')$ [Eqs. (60) and (70)] by replacing the lower limit of the integration $k_F|\psi'|$ approximately by $|y|$, which is, however, a solution of (74), i.e., $|y| = \frac{1}{2c}(1-\sqrt{1-4ck_F|\psi'|})$, but it is not the linear function of $|\psi'|$ in that $|y| = k_F|\psi'|$. This replacement is done in order to introduce in the relationship of $f(\psi')$ with $F(y)$ in (70) and (72) the lower limit in the integral for $F(y)$ to be $|y|$ (as in the YS) where, however, the correct relationship of $|y|$ with $|\psi'|$ [Eq. (74)] is accounted for. In Fig. 4 we give the results for $f(\psi')$ from Eq. (75) using the NMD from the YS analysis [13,14] [Eqs. (9)–(11)] and from the approach [25] within the LFD method [Eqs. (76)–(79), (81), and (82)]. One can see that the NMD from the YS analysis [Eqs. (9)–(11)] gives a good description of $f(\psi')$ for ^{56}Fe in the case of $q = 1000$ MeV/c for ψ' values of $-1.10 \leqslant \psi' \leqslant 0$ (for which $y < 0$ and $|y| \leqslant 1/(2c)$ at $c = 0.144$ fm). The scaling function $f(\psi')$ calculated by $n(k)$ from the LFD is in agreement with the data for $-0.5 \lesssim \psi' \leqslant 0$, while in the region $-1.1 \leqslant \psi' \leqslant -0.5$ it shows a dip in the interval $-0.9 < \psi' \leqslant -0.6$. The difference in the behavior of $f(\psi')$ in these two cases reflects the difference of the momentum distributions of YS and LFD in the interval $1.5 \lesssim k \lesssim 2.5$ fm^{-1}. The $n(k)$ of the LFD has a dip around $k \approx 1.7$ fm^{-1} below the curve of $n(k)$ from the YS analysis.

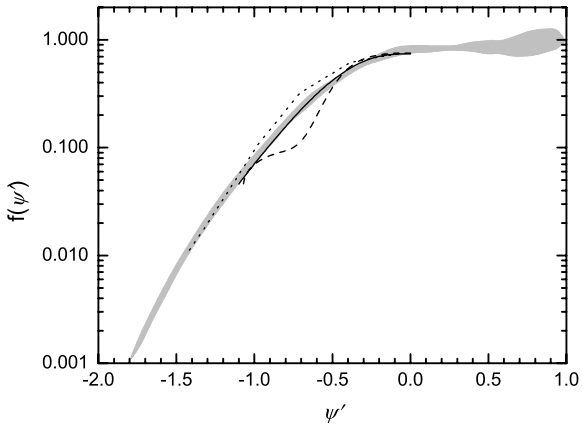

FIG. 4. The ψ'-scaling function $f(\psi')$ at ^{56}Fe and $q = 1000$ MeV/c calculated from Eq. (75) using $n(k)$ from (i) the $y_{\rm CW}$-scaling analysis [13,14] [Eqs. (9)–(11)] (solid line) and (ii) the approach [25] within the LFD method [Eqs. (76)–(79), (81), and (82)] (dashed line). The CDFM result obtained using Eqs. (45) and (46) is given by the dotted line. The experimental data given by the shaded area are from [21].

IV. CONCLUSIONS

1. The main aim of our work was to study the nucleon momentum distributions from the experimental data on inclusive electron scattering from nuclei that have shown the phenomenon of superscaling. For this purpose we made an additional extension of the coherent density fluctuation model in order to express the ψ'-scaling function $f(\psi')$ explicitly in terms of the nucleon momentum distribution for realistic finite systems. This development is a natural extension of the relativistic Fermi gas model. In this way $f(\psi')$ can be expressed equivalently by means of both density and momentum distributions. In [9] our results on $f(\psi')$ were obtained on the basis of the experimental data on the charge densities for a wide range of nuclei. In the present work we discuss the properties of $n(k)$ that correspond to the results for $f(\psi')$ obtained in the CDFM. Thus we show how both quantities, the density and the momentum distribution, are responsible for the scaling behavior in various nuclei.
2. In addition to the work presented in Ref. [9], the scaling function $f(\psi')$ is calculated here in the CDFM at $q = 1560$ MeV/c. The comparison with the data from [22] shows superscaling for negative values of ψ' including $\psi' < -1$, in contrast to the RFG model where $f(\psi') = 0$ for $\psi' \leqslant -1$.
3. The y-scaling function $F(y)$ is defined in the CDFM on the basis of the RFG relationships. The calculations of $F(y)$ are performed in the model using three different momentum distributions: from the CDFM, from the y-scaling analyses [13,14], and from the theoretical approach based on the light-front dynamics method [25]. Comparing the results of the calculations for ^{4}He and ^{56}Fe nuclei with the experimental data, we show the sensitivity of the calculated $F(y)$ to the peculiarities of the three $n(k)$ in different regions of momenta.
4. An approximate relationship between $f(\psi')$ and $F(y)$ is established. It is shown that the momentum distribution $n_{\rm CW}$ for ^{56}Fe from the y-scaling studies in [13,14] can describe to a large extent the empirical data on $f(\psi')$ for $q = 1000$ MeV/c. We point out that the studies of the interrelation and the comparison between the results of the ψ'- and y-scaling analyses have to account for the correct nonlinear dependence of ψ' on the y-scaling variable, which reflects the dependence on the missing energy.
5. The regions of momenta in $n(k)$ that are mainly responsible for the description of the y- and ψ'-scaling are estimated. The existing data on the y- and ψ'-scaling are shown to be informative for the momentum distribution $n(k)$ at momenta up to $k \lesssim 2$–2.5 fm^{-1}. Further experiments are necessary in studies of the high-momentum components of the nucleon momentum distribution.

ACKNOWLEDGMENTS

One of the authors (A.N.A.) is grateful for the warm hospitality of the Faculty of Physics of the Complutense University of Madrid and the Instituto de Estructura de la Materia, CSIC, and for support during his stay there from the State Secretariat of Education and Universities of Spain (N.Ref.SAB2001-0030). Four of the authors (A.N.A., M.K.G., D.N.K., and M.V.I.) are thankful to the Bulgarian National Science Foundation for partial support under Contract Nos. Φ-905 and Φ-1416. This work was partly supported by funds provided by DGI of MCyT (Spain) under Contract Nos. BFM 2002-03562, BFM 2000-0600, and BFM 2003-04147-C02-01 and by the Agreement (2004 BG2004) between the CSIC (Spain) and the Bulgarian Academy of Sciences.

[1] O. Bohigas and S. Stringari, Phys. Lett. **B95**, 9 (1980).
[2] M. Jaminon, C. Mahaux, and H. Ngô, Phys. Lett. **B158**, 103 (1985).
[3] E. Moya de Guerra, P. Sarriguren, J. A. Caballero, M. Casas, and D. W. L. Sprung, Nucl. Phys. **A529**, 68 (1991).
[4] A. N. Antonov, P. E. Hodgson, and I. Zh. Petkov, *Nucleon Momentum and Density Distributions in Nuclei* (Clarendon Press, Oxford, 1988).
[5] A. N. Antonov, P. E. Hodgson, and I. Zh. Petkov, *Nucleon Correlations in Nuclei* (Springer-Verlag, Berlin-Heidelberg-New York, 1993).
[6] A. N. Antonov, V. A. Nikolaev, and I. Zh. Petkov, Bulg. J. Phys. **6**, 151 (1979); Z. Phys. A **297**, 257 (1980); **304**, 239 (1982).
[7] A. N. Antonov, V. A. Nikolaev, and I. Zh. Petkov, Nuovo Cimento A **86**, 23 (1985).
[8] A. N. Antonov, E. N. Nikolov, I. Zh. Petkov, Chr. V. Christov, and P. E. Hodgson, Nuovo Cimento A **102**, 1701 (1989);

A. N. Antonov, D. N. Kadrev, and P. E. Hodgson, Phys. Rev. C **50**, 164 (1994).
[9] A. N. Antonov, M. K. Gaidarov, D. N. Kadrev, M. V. Ivanov, E. Moya de Guerra, and J. M. Udias, Phys. Rev. C **69**, 044321 (2004).
[10] G. B. West, Phys. Rep. **18**, 263 (1975).
[11] C. Ciofi degli Atti, E. Pace, and G. Salme, Phys. Lett. **B127**, 303 (1983).
[12] C. Ciofi degli Atti, E. Pace, and G. Salme, Phys. Rev. C **43**, 1155 (1991).
[13] C. Ciofi degli Atti and G. B. West, Phys. Lett. **B458**, 447 (1999).
[14] Claudio Ciofi degli Atti and Geoffrey B. West, nucl-th/9702009 (1997).
[15] D. Day, J. S. McCarthy, T. W. Donnelly, and I. Sick, Ann. Rev. Nucl. Part. Sci. **40**, 357 (1990).
[16] I. Sick, D. Day, and J. S. McCarthy, Phys. Rev. Lett. **45**, 871 (1980).
[17] E. Pace and G. Salme, Phys. Lett. **B110**, 411 (1982).
[18] C. Ciofi degli Atti and S. Simula, Phys. Rev. C **53**, 1689 (1996).
[19] W. M. Alberico, A. Molinari, T. W. Donnelly, E. L. Kronenberg, and J. W. Van Orden, Phys. Rev. C **38**, 1801 (1988).
[20] M. B. Barbaro, R. Cenni, A. De Pace, T. W. Donnely, and A. Molinari, Nucl. Phys. **A643**, 137 (1998).
[21] T. W. Donnelly and Ingo Sick, Phys. Rev. C **60**, 065502 (1999).
[22] T. W. Donnelly and I. Sick, Phys. Rev. Lett. **82**, 3212 (1999).
[23] C. Maieron, T. W. Donnelly, and Ingo Sick, Phys. Rev. C **65**, 025502 (2002).
[24] M. B. Barbaro, J. A. Caballero, T. W. Donnelly, and C. Maieron, Phys. Rev. C **69**, 035502 (2004).
[25] A. N. Antonov, M. K. Gaidarov, M. V. Ivanov, D. N. Kadrev, G. Z. Krumova, P. E. Hodgson, and H. V. von Geramb, Phys. Rev. C **65**, 024306 (2002).
[26] H. Meier-Hajduk, Ch. Hajduk, P. U. Sauer, and W. Theis, Nucl. Phys. **A395**, 332 (1983); C. Ciofi degli Atti, E. Pace, and G. Salme, Phys. Rev. C **21**, 805 (1980).
[27] O. Benhar, A. Fabrocini, and S. Fantoni, Nucl. Phys. **A550**, 201 (1992).
[28] J. J. Griffin and J. A. Wheeler, Phys. Rev. **108**, 311 (1957).
[29] V. V. Burov, D. N. Kadrev, V. K. Lukyanov, and Yu. S. Pol', Phys. At. Nucl. **61**, 525 (1998).
[30] H. De Vries, C. W. De Jager, and C. De Vries, At. Data Nucl. Data Tables **36**, 495 (1987).
[31] J. D. Patterson and R. J. Peterson, Nucl. Phys. **A717**, 235 (2003).
[32] J. Carbonell and V. A. Karmanov, Nucl. Phys. **A581**, 625 (1995).
[33] J. Carbonell, B. Desplanques,V. A. Karmanov, and J.-F. Mathiot, Phys. Rep. **300**, 215 (1998).
[34] P.-O. Löwdin, Phys. Rev. **97**, 1474 (1955).
[35] M. V. Stoitsov, A. N. Antonov, and S. S. Dimitrova, Phys. Rev. C **47**, R455 (1993); **48**, 74 (1993).
[36] Dino Faralli, Claudio Ciofi degli Atti, and Geoffrey B. West, in *Proceedings of Second International Conference on Perspectives in Hadronic Physics, ICTP, Trieste, Italy, 1999*, edited by S. Boffi, C. Ciofi degli Atti, and M. M. Gainnini (World Scientific, Singapore, 2000), p. 75.